



Measurement of size-fractionated atmospheric particulate matter and associated polycyclic aromatic hydrocarbons in Mumbai, India, and their dry deposition fluxes

M. Tiwari¹ · S. K. Sahu¹ · T.D. Rathod¹ · R. C. Bhangare¹ · P.Y. Ajmal¹ · A Vinod Kumar¹

Received: 27 February 2020 / Accepted: 10 June 2020 / Published online: 23 June 2020
© Springer Nature B.V. 2020

Abstract

Size-fractionated particulate matter (PM), associated polycyclic aromatic hydrocarbons (PAHs), and their dry deposition fluxes were measured in a coastal urban environment of Mumbai, India. PM samples were collected using a variable configuration cascade impactor (VCCI) with 11 size fractionation stages. Dry deposition samples were collected using a round-bottomed PVC tray. High-performance liquid chromatography (HPLC) was used for the identification and quantification of PAHs in samples. PM were observed to range between 58 and 130 $\mu\text{g m}^{-3}$, with a mean dry deposition flux of 1298 $\text{mg m}^{-2} \text{day}^{-1}$. Observed PM concentrations during the sampling period were found to be well above the WHO Air Quality Guidelines. A strong linear correlation was observed between the gravitational settling velocities and estimated dry deposition velocities for PM. Concentrations of PAHs associated with PM were observed to be in the range 101–145 ng m^{-3} while their dry deposition fluxes varied from 1008 to 1160 $\text{ng m}^{-2} \text{month}^{-1}$. The molecular diagnostic ratios (MDRs) indicated that sources of PAHs in the study area were petrogenic as well as non-traffic. The dry deposition velocities calculated for PAHs were in the order of $10^{-4} \text{ cm s}^{-1}$ to $10^{-3} \text{ cm s}^{-1}$ in the entire size range.

Keywords PAHs · Particulate matter · Dry deposition · Deposition velocity · Molecular diagnostic ratio

Introduction

Polycyclic aromatic hydrocarbons (PAHs) are a group of organic compounds containing two or more fused rings (Nasibande et al. 2019). These compounds have low solubility in water and have preferential adsorption on solid and carbonaceous materials in the environment. PAHs are ubiquitous in the environment with several studies reporting their presence in the air, sediments, soils, and wastewater sludge (Kim et al. 2013; Tiwari et al. 2017a; Ncube et al. 2018). Atmospheric PAHs are contaminants of concern in urban air as they are carcinogenic and mutagenic (Garrido et al. 2014). PAHs are produced from

incomplete combustion or pyrolysis of carbon-containing materials such as fossil fuels and biomass. Generally, PAHs are produced from anthropogenic emissions such as industrial production, transportation, and waste incineration. The predominant source of PAHs in an urban environment is vehicular emissions (Khaiwal et al., 2008; Gupta et al. 2011). Other anthropogenic sources of PAHs consist of residential heating; coal gasification and liquefying plants; carbon black, coal-tar pitch, and asphalt production; catalytic cracking towers; and related activities in petroleum refineries (Abdel-Shafya and Mansour 2016). PAHs are also subjected to gas and particle-phase partitioning in ambient air (Shen et al. 2011), which depends on particle sizes, PAH species, and meteorological parameters. The size distribution of particles onto which PAH attaches plays a critical role in their impact on health and their fate in the environment. High molecular mass PAHs predominantly accompany fine atmospheric particulate matter ($\text{PM}_{2.5}$ refers to atmospheric particulate matter (PM) that has an aerodynamic diameter of less than 2.5 μm) (Wu et al. 2014; Tong et al. 2019). As deposition of particles in the respiratory tract through inhalation depends on their size, fine particles with PAHs can penetrate deep into the human respiratory system and exhibit adverse health effects (Zhang et al. 2012; Burkart et al. 2013; Tiwari et al. 2017).

Electronic supplementary material The online version of this article (<https://doi.org/10.1007/s11869-020-00849-z>) contains supplementary material, which is available to authorized users.

✉ S. K. Sahu
sksahu@barc.gov.in

¹ Environmental Monitoring and Assessment Division, Health Safety and Environment Group, Bhabha Atomic Research Center, Mumbai 400085, India

Over the previous decade, several measurements of size distributions of atmospheric PAHs have been reported from various regions around the world (Kaupps and McLachlan 1999; Lee et al. 2008; Wang et al. 2009; Gupta et al. 2011, Gnauk et al. 2011; Phoothiwut and Junyapoon 2013; Shi et al. 2015; Pooltawee et al. 2017). Due to persistence in the environment and their semi-volatile nature, PAHs deposited onto soils, vegetation, and watersheds can be re-emitted to the atmosphere. There is rising evidence that low molecular weight PAHs can be formed naturally in soils and volatilize to the atmosphere and can contribute to atmospheric concentration (IARC 1991; Cincinelli et al. 2007). Increasing concentration of PAHs in the atmosphere is concerning for human health. Various national and international bodies have proposed air quality standards for some high toxic PAHs that aim to reduce atmospheric emissions and exposure (Katsoyiannis et al. 2011). Methodologies for PAH source identification and apportionment comprise various emission inventory modeling tactics, multivariate statistics, and alternatively to them, the use of markers and diagnostic ratios. Selected PAH concentration ratios of ambient samples and source emissions are often used as diagnostic tools to recognize the sources of PAHs (Dvorská et al. 2011).

Dry deposition is a crucial route for the removal of gases and particles from the atmosphere, via diffusion, impaction, or gravitational settling onto vegetation, soil, and water bodies, followed by attachment to these materials. The dynamics governing dry deposition of a gaseous species or a particle are atmospheric turbulence, physio-chemical properties of the depositing species, and the nature of the depositing surface (Seinfeld and Pandis 2006). Dry deposition is a multifaceted process that is governed by the chemical properties of PM and their sources, meteorological parameters, and surface topographies. The deposition of particles from the atmosphere to the Earth's surface is also steered by different forces such as friction drag and terrain-based flow alterations (Stull 2012). To understand the factors governing dry deposition process, it is necessary to estimate the residence time of atmospheric particulates, which impacts their long-range transport, transboundary fluxes, and associated climate effects (Pryor et al. 2008). For PM, their size, density, and shape regulate their adsorption on surfaces. An inert surface may forbid absorption or adsorption of some gases, while a flat surface may lead to particle bouncing-off. Complex natural surfaces, such as vegetation, show large surface variability often challenging to describe theoretically, generally enhance dry deposition due to their surface non-uniformity (Seinfeld and Pandis 2006). Dry deposition is slow for particles of diameter 0.1–1 μm (fine), but dominant for larger (coarse) and smaller (ultrafine) particles. The dry deposition fluxes of various substances appear to be governed by large particles, even for compounds with an extremely low association in this size range (Birgül et al., 2011). Particle sizes also determine the wet removal of the PM and the associated chemicals. Measurement of particle size distributions in and under the clouds, before and

after precipitation events indicates a marked size dependence for the wet deposition efficiencies for atmospheric particles (Radke et al. 1980; Chate et al. 2003). PAHs such as phenanthrene, fluoranthene, pyrene, chrysene, benzo[b]fluoranthene, and benzo[k]fluoranthene were identified to be the dominant PAHs associated with the deposited aerosol particles (Wang et al. 2014). Given the significance of particle size distribution for the atmospheric fate of organic substances, minimal information is available on this subject. As the particle size determines most of the properties of PM, a study of size-fractionated particle-bound substance is relevant for estimating their input into ecosystems through dry deposition.

The present study aims to measure particle size distributions of PM and associated PAHs and dry deposition sampling in Mumbai, India, from March 2018 to May 2018. The objectives of the study can be listed as follows: (i) collection of the PM using variable configuration cascade impactor (VCCI) (ii) analysis of the PAH distribution among the different size fraction (iii) collection and analysis of dry deposition samples for PM and PAHs (iv) calculation of deposition velocity and fluxes for PM and PAHs.

Materials and methods

Study area

Size-fractionated PM samples were collected at Trombay (19.0° N, 72.9° E), a coastal urban environment of Mumbai. The sampling site is boarded by the Arabian Sea on one side (east) and by an industrial area (separated by a hill) on the other side (west). The sampling site is close to various industries, viz., coal- and oil-burning power plant, oil refineries, a fertilizer plant complex, and automobile, metallurgical, chemical, paint, and small metal industry plants in the west direction. On the east, crossing the Trans Thane Creek (TTC), several other industrial areas are located, e.g., Maharashtra Industrial Development Corporation, Taloja, Turbhe, Trans Thane Creek, and Jawaharlal Nehru Port Trust (JNPT, one of the largest ports in India, handling various chemicals, petroleum products, crude oil, and other merchandises). Mumbai receives significant rainfall during the monsoon (June–August), with an annual average of 2240 mm. The wind speed at the sampling site varied from 0.5 to 7.5 m s^{-1} in summer and winter and was found to be as high as 17 m s^{-1} in the monsoon (Police et al. 2018; Tiwari et al. 2019).

Sampling

Size-segregated PM samples were collected from March to May 2018, using a custom-built variable configuration cascade impactor (VCCI). Details of VCCI sampler are described elsewhere (Tiwari et al. 2013; Singh et al. 2010). Air sampling

was carried out on a rooftop of a 10-m high building at Trombay, Mumbai. Discs of glass fiber filter paper (EPM 2000, Whatman) were used for size-segregated PM collection. Previously, numbered glass fiber papers were dried in an oven at 400 °C for 6 h to remove possible organic contaminants and stored in a desiccator for 24 h before weighing. Sampling air was drawn through the impactor at a flow rate of 0.6 m³ h⁻¹. The size ranges (in μm) collected from the different stages of cascade impactor were > 21.3, 21.3–15.1, 15.1–11.2, 11.2–7.38, 7.38–5.47, 5.47–2.23, 2.23–1.13, 1.13–0.75, 0.75–0.50, 0.50–0.30, 0.30–0.10, and < 0.10. Sampling was carried out twice a week (30 h to each, 19 m³ of air). The images of VCCI and collected PM samples are shown in Fig. 1. Filter papers were again weighed after the collection, and the mass difference was used to calculate mass loading in each stage of the impactor.

During the sampling period, rainfall is minimum, so only dry deposition samples were collected. Samples were collected using a custom-built round bottom PVC tray (bottom diameter 30 cm, height 25 cm). This method of sample collection and processing has been adopted as per Terzi and Samara 2005. Samples were collected at a distance of 100 m from the VCCI sampling location. The dry deposition samples were collected once on a bi-weekly basis by rinsing PVC tray with double distilled water after the removal of any visual contamination like bugs, birds, and droppings. The walls of the PVC tray were further wiped with glass wool to collect all the samples. Dry deposition samples were stored in the refrigerator at – 20 °C until analysis.

Sample extraction and instrumental analysis

After collecting the size-fractionated PM, the glass fiber filter papers were chemically processed for the extraction of PAHs. The solvents and reagents used were of HPLC grade purity. Amber glassware was used during the extraction and analysis

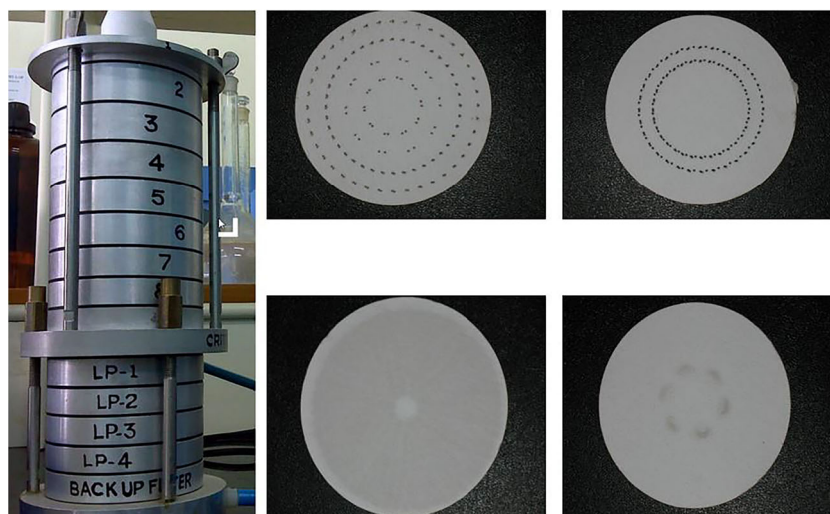
of the samples to inhibit photo-degradation of PAHs. The glass fiber filter paper samples were cut into small pieces and were subjected to ultra-sonication in 40 mL n-hexane for 1 h. The extracts were filtered through Whatman 542 filter paper. The filtrates were kept for natural evaporation in a fume hood until the volume reduced to 1 mL. Extracted samples were passed through a silica column of 10 cm × 2 cm size with 50 mL of n-hexane and dichloromethane at the ratio of 1:1 (v/v) as clean up before chromatographic analysis (Tiwari et al. 2013). Samples of dry deposition (as water suspension) were filtered through C-18 SPE cartridges (1 g). Cartridges were subjected to ultra-sonication in 60 mL acetonitrile for 1 h. Further processing was similar to PM extraction and clean up procedure as described above.

The identification and quantification of PAHs were performed on a high-performance liquid chromatography (HPLC) system (Jasco X-LC). HPLC system consists of a binary pump (model: Jasco X-LC 3185PU) with an autosampler (model: Jasco X-LC 3159AS), with a multi-wavelength detector (model: Jasco MD-2015plus). Jasco LC-NETII/ADC was used for data processing and ChormNAV as acquisition software. The detector wavelength was set at 254 nm, which shows maximum absorbance response to the polycyclic aromatic hydrocarbons (Sahu et al. 2009). The analysis was carried out in reverse phase and isocratic mode (acetonitrile:H₂O, 70:30), C-18 column (5 μm size fully porous Octadecyl silane packing, Merck Germany), 250 mm × 4.6 mm (i. d.) with a C-18 guard column. A standard synthetic mixture of PAHs (Supelco, USA) was used as an external standard.

Data analysis

The most important surface properties which determine the dry deposition process include chemical and biological reactivity, geometry and roughness, terrain characteristics, and

Fig. 1 Variable configuration cascade impactor (VCCI) and photographs of selected stage samples



wetness. Natural surfaces, such as vegetation, generally facilitate dry deposition (Pacyna 2008). Dry deposition is the portion of the total deposition in dry weather through processes such as settling, impaction, and adsorption. Dry deposition is usually quantified in terms of the flux F , which is a function of the dry deposition velocity (v_d) and concentration of a chemical in the air (C):

$$v_d(z) = \frac{F}{C(z)} \quad (1)$$

Resistance models for dry deposition are used to calculate the dry deposition velocity based on the resistance to transport for each step in the process:

$$v_d = \frac{1}{r_a + r_b + r_c} + v_g \quad (2)$$

where r_a is the resistance to aerodynamic transport, r_b is the resistance to the transport through the boundary sublayer, r_c is resistance to the collection by the surface, and v_g is gravitational settling velocity.

$$v_g = \frac{\rho_p D_p^2 g C_c}{18 \mu} \quad (3)$$

$$C_c = 1 + \frac{2\lambda}{D_p} \left[1.257 + 0.4 \exp\left(-\frac{1.1D_p}{2\lambda}\right) \right] \quad (4)$$

where ρ_p is particle density, D_p is particle diameter, μ is the viscosity of air, and C_c is the slip correction coefficient defined in Eq. (4). The viscosity of air as a function of temperature is defined as Eq. (5).

$$\mu = 1.8 \times 10^{-5} \left(\frac{T}{298} \right)^{0.85} \quad (5)$$

where T is expressed in K and λ is the air mean free path (Seinfeld and Pandis 2006). The three transport processes (aerodynamic transport, the transport through the boundary sublayer, and the resistance to the collection by the surface) must be considered to model the dry deposition of fine particles. The aerodynamic transport of fine particles occurs by turbulent diffusion and gravitational sedimentation with a little influence of Brownian diffusion. The turbulent diffusion coefficient of a given chemical above the vegetation canopy is assumed to be the same as the kinetic eddy viscosity of the air. Particles can also be transported in the air by turbulent bursts, such as eddies from the free atmosphere or eddies created by the surface roughness. The rate of particle transport by turbulent bursts is comparable with the rate of aerodynamic transport in the region and is not affected by the viscous sublayer (Mohan 2016). Meteorological dynamics, such as temperature, wind speed, and relative humidity, can affect the stability and particle friction velocity in the atmosphere. Deposition

velocity and concentration of the PM are also intensely affected by friction and atmospheric stability classes (Connan et al. 2013, Wu et al. 2018). Thus, one can determine that meteorological parameters have a significant impact on the deposition velocity. The graphical illustrations of the atmospheric PM and PAHs data were constructed with Microsoft Excel (2016) and Origin 8.0. Both of them were used to calculate the measure of central tendency and dispersion in air PM and PAH data.

Quality control and quality assurance

Laboratory blanks (PVC tray, GF filters) were estimated to evaluate potential contaminations of dry deposition and PM samples. PAH levels were below the analytical detection limit in field and laboratory blanks. Several dilutions corresponding to 0.1–100 ng absolute of synthetic standard mixture of styrene (STY), naphthalene (NAP), acenaphthylene (ACY), acenaphthene (ACE), fluorene (FLU), anthracene (ANT), fluoranthene (FLUO), pyrene (PYR), benzo (a) anthracene (BaA), chrysene (CHY), benzo(b)fluoranthene (BbF), benzo(k)fluoranthene (BkF), benzo(a)pyrene (BaP), benzo(ghi)perylene (BghiP), indeno(1,2,3-cd)pyrene (IND) (purchased from Supelco, Bellefonte, USA) were used for determining the retention data and for studying the linearity of the UV-vis detector. The detection limits and limits of quantification (LOQs) for each PAHs were calculated as the concentrations at which the signal-to-noise ratios were three and ten, respectively. For confirmation of PAH compounds, UV-Vis spectra (200–800 nm) of each PAHs were generated using standards and saved for comparison in a spectral library. In samples, spectra of target PAHs were matched with the library in addition to retention time data before quantification based on maximum absorbance. The recovery efficiencies were determined by spiking filter paper samples with PAH standard mixture. The performance evaluation of dry deposition extraction procedure and atmospheric particulate phase PAH concentration was estimated using NIST 1649 “urban dust” for target compounds. The mean recoveries were found to vary between 82 and 94% for PAHs in dry deposition and atmospheric particulate phase (direct analysis). Details on quality control and assurance adopted in this study are described elsewhere (Tiwari et al. 2013; Tiwari et al. 2017).

Results and discussion

Size-fractionated atmospheric PM

Monthly averages of size-fractionated mass concentration for the atmospheric PM at the sampling site (Trombay, Mumbai) are presented in Table 1. Here, we observed that total particulate mass concentrations vary between 58.2 ± 7.3 and $130 \pm$

Table 1 Size-fractionated mass concentration of PM ($\mu\text{g m}^{-3}$) using variable configuration cascade impactor (VCCI)

Size range (micron)	March ($\mu\text{g m}^{-3}$)	April ($\mu\text{g m}^{-3}$)	May ($\mu\text{g m}^{-3}$)
> 21.3 μm	17.9 \pm 2.1	9.1 \pm 2.5	6.6 \pm 0.3
21.3–15.1 μm	1.8 \pm 0.8	6.6 \pm 0.1	6.6 \pm 0.5
15.1–11.2 μm	5.3 \pm 0.5	3.6 \pm 0.3	3.9 \pm 0.2
11.2–7.38 μm	5.4 \pm 0.4	3.8 \pm 1.2	2.6 \pm 0.6
7.38–5.47 μm	8.9 \pm 1.2	4.9 \pm 1.6	6.6 \pm 0.8
5.47–2.23 μm	51.8 \pm 5.6	20.4 \pm 4.5	15.9 \pm 2.3
2.23–1.13 μm	21.4 \pm 3.1	9.1 \pm 2.5	6.6 \pm 1.3
1.13–0.75 μm	3.6 \pm 0.9	2.1 \pm 0.5	2.6 \pm 0.2
0.71–0.50 μm	1.8 \pm 0.3	1.5 \pm 0.1	1.3 \pm 0.2
0.50–0.30 μm	1.7 \pm 0.5	2.3 \pm 1	1.3 \pm 0.1
0.30–0.10 μm	8.9 \pm 1.2	1.5 \pm 0.1	1.3 \pm 0.3
< 0.10 μm	1.8 \pm 0.3	2.9 \pm 0.3	2.6 \pm 0.2
Total	130 \pm 17	68.2 \pm 14.9	58.2 \pm 7.3

17.1 $\mu\text{g m}^{-3}$ during the sampling period, and they decreased from March to May. A similar trend of $\text{PM}_{2.5-10}$ and $\text{PM}_{2.5}$ was observed in our previous study for this sampling site (Police et al. 2018). Most of the mass loading was observed in 2.23–5.47 μm size bin (coarse fraction) for all 3 months. The total particulate load observed in April was almost half of that observed in March. This may be due to spring to summer transition of season (rise in temperature). For March, the mass concentration data were exceeding the annual limit prescribed by Indian National Ambient Air Quality Standards (NAAQS) (i.e., 40 $\mu\text{g m}^{-3}$ for $\text{PM}_{2.5}$ and 100 $\mu\text{g m}^{-3}$ for PM_{10}), while for other months, the concentrations were under the prescribed limits (CPCB 2009). Observed PM concentrations during the sampling period were found to be well above the WHO Air Quality Guideline values, i.e., the annual mean of 10 $\mu\text{g m}^{-3}$ for $\text{PM}_{2.5}$ and 20 $\mu\text{g m}^{-3}$ for PM_{10} (WHO 2018). Vigilantly, these compared data were monthly average, and an annual average data could have given a better understanding of PM loads in ambient air while comparing with guideline values.

The size-fractionated mass concentration data were further categorized into four groups of particle sizes: (i) ultrafine ($\text{PM}_{0.1}$), (ii) fine ($\text{PM}_{2.23}$), (iii) coarse ($\text{PM}_{2.23-11.2}$), and (iv) suspended PM ($\text{PM}_{>11.2}$). The percentage distribution of mass concentration during the 3 months of sampling is shown in Table 2. Most of the mass was found in coarse fraction ($\text{PM}_{2.23-11.2}$) mode, which is found to be between 43 and 51% of the total mass concentration. The reason for the high abundance of coarse mode particles may be natural sources such as dust and sea salt present at the sampling site (Police et al. 2018; Koulouri et al. 2008). The total abundance of fine ($\text{PM}_{2.23}$) and suspended ($\text{PM}_{>11.2}$) mode PM was found approximately to be in the range of 19 to 29% of the total mass concentration. The contribution of ultrafine particulates

Table 2 Percentage distribution of ultrafine ($\text{PM}_{0.1}$), fine ($\text{PM}_{2.23}$), coarse ($\text{PM}_{2.23-11.2}$), and suspended particulate matter ($\text{PM}_{>11.2}$) fractions in total PM

	March (%)	April (%)	May (%)
$\text{PM}_{0.1}$	1.0	4.2	5.2
$\text{PM}_{2.23}$	28.9	24.4	25.9
$\text{PM}_{2.23-11.2}$	50.9	42.9	49.3
$\text{PM}_{>11.2}$	19.2	28.5	19.6

($\text{PM}_{0.1}$) was minimum among all, i.e., 1 to 5% to the total mass concentration. Table 2 also indicates a minor variation in size fraction of PM over the sampling period, as variation in percentage contribution of ultrafine ($\text{PM}_{0.1}$), fine ($\text{PM}_{2.23}$), coarse ($\text{PM}_{2.23-11.2}$), and suspended PM ($\text{PM}_{>11.2}$) fractions to the total concentration of PM is not significant.

Dry deposition flux of atmospheric PM

The dry deposition flux of atmospheric PM was calculated by dividing the mass loading on the collection plate by the collection area and sampling time. The average dry deposition flux observed during the sampling period was $12.9 \pm 2.1 \text{ mg m}^{-2} \text{ day}^{-1}$. Monthly average dry depositions were 15.4 ± 0.8 , 12.2 ± 0.4 , and $11.3 \pm 0.4 \text{ mg m}^{-2} \text{ day}^{-1}$ for the sampling periods March, April, and May, respectively. They are comparable to the deposition fluxes reported for Lake Michigan in the USA, which were measured using Eagle II automatic dry deposition collectors (Shahin et al. 2010; Caffery 1997). Furthermore, the dry deposition fluxes of the PM depend on their atmospheric concentrations. Thus, measured fluxes and concentrations should have a strong correlation (Yi et al. 2006). To estimate the inter-dependency of mass concentration and deposition flux, these two variables were plotted against each other. Mass concentration data were averaged throughout the dry deposition collection period (15 days) for better statistical estimation. Positive linear correlation ($r = 0.98$, $p < 0.05$) has been observed between mass concentration and dry deposition flux of the atmospheric PM.

Dry deposition fluxes for size-fractionated atmospheric PM were also calculated using their gravitational settling velocities (considering the best estimate for the deposition velocity) and ambient concentrations. The calculated values are shown in Table 3 for an individual sample. The gravitational settling velocity V_g was calculated using Eq. (3). Also, the slip correction coefficient (C_c) was incorporated in the calculation using Eq. (4) for better estimation. In this calculation, it was assumed that meteorological conditions were stable throughout the sampling period and various resistances such as aerodynamic transport, boundary sublayer, and collection surface were not affecting the process. Exceptional cases where dry

deposition velocity could be considered as an actual velocity are when gravitational settling controls the deposition. In the small particles, they are the same as that for large size particles (Zhang et al. 2001). Based on model simulation, the universal curve of dimensionless dry deposition velocity was observed to be in the range of 10^{-4} to 10^{-7} m s⁻¹ for all the PM sizes monitored in this study (0.1 to > 21.3 μm) (Hussein et al. 2012), which are in good agreements with the calculated gravitational settling velocities, and shown in Table 3.

Calculated and observed dry deposition fluxes showed a positive linear correlation with the correlation coefficient (*r*) of 0.97. Theoretically, particles with minute differences in their dry deposition velocities should have a better correlation between their measured flux and concentration, as the change in the flux is primarily due to the change in the concentration of the PM. Conversely, two factors might reduce the correlation. The first factor is related to the measurement errors caused by the uncertainties of the apparatuses that are used for the collection of atmospheric PM, which subsequently lead to analytical artifacts. The second factor is the rationality of the assumption that a surrogate surface represents the natural surface in the collection of pollutants (Mohan 2016).

Dry deposition velocities (v_d) for PM were calculated using Eq. (1), using the observed dry deposition flux. The monthly average dry deposition velocities were 0.14, 0.20, and 0.22 cm s⁻¹, respectively, for March, April, and May. Shi et al. (2013) conducted a study on concentration and deposition flux of atmospheric particulate nutrients over the Yellow Sea. Dry deposition velocity for total suspended particulates in their study was reported as 0.27 cm s⁻¹ during regular days (no dust storm periods) of the sampling period, which is comparable to our observed values.

Size-fractionated particulate PAHs

Concentrations of PAHs (\sum_{15} and styrene) were measured in size-segregated ambient air particulates. The monthly average concentrations of individual PAHs in each size fractions are presented in supplementary Table S1 to Table S3. Two PAHs, viz., chrysene and benzo(a)anthracene are reported together due to their chromatographic interferences. The total particulate phase monthly average concentrations of \sum_{15} PAHs were 145.2 ± 32.3 , 122.3 ± 20.3 , and 101.1 ± 21.8 ng m⁻³ for March, April, and May, respectively. The trend of PAH concentration was very similar to PM concentration in air, in the order March > April > May. Monthly size-fractionated \sum_{15} PAH concentrations (with styrene) are presented in Fig. 2. Figure 2 reveals that 46 to 77% of \sum_{15} PAHs were associated with fine PM, i.e., PM_{1.13}. PAHs associated with an inhalable fraction of PM were in the range of 70 to 90% of \sum_{15} PAHs during the sampling period. This association of the PAHs with fine PM could be due to high surface to volume ratio and more organic content in the fine fraction of PM (Sheu et al. 1997).

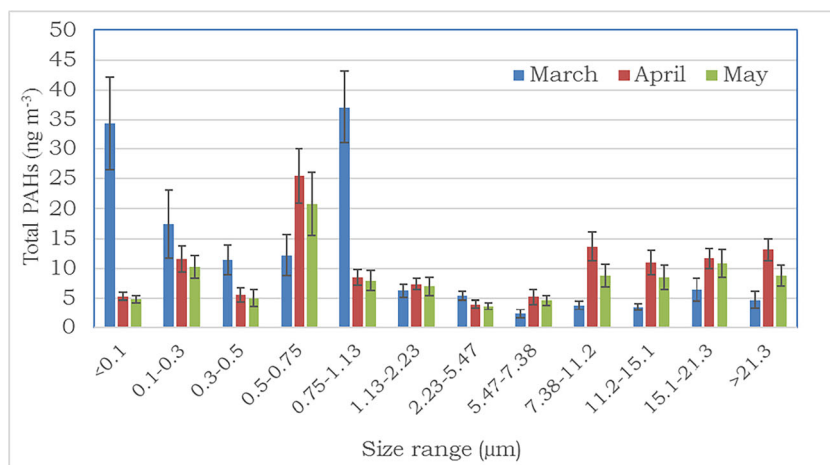
Target PAHs compounds were categorized in three groups according to the number of structural rings: (i) 2 and 3-ring PAHs (NAP, ACY, ACE, FLU, and ANT), (ii) 4-ring PAHs (FLUO, PYR, BaA, and CHR), and (iii) 5 and 6-ring PAHs (DBA, IND, BghiP). The order of ring wise PAHs abundance in ambient air was observed to be 2 + 3-ring PAHs > 5 + 6-ring PAHs > 4-ring PAHs. Two and 3-ring PAHs were highest in abundance, and their concentrations varied between 2.2 and 13 ng m⁻³. The particulate phase concentrations ranges of 4-ring PAHs and 5 + 6-ring PAHs were 0.1 to 2 ng m⁻³ and 0.7 to 3.8 ng m⁻³, respectively. Percentage contributions of 2 + 3-ring, 4-ring, and 5 + 6-ring PAHs were 72.5%, 8.2%, and

Table 3 Calculation of size-fractionated deposition fluxes using gravitational settling velocity

Size range (μm)	Geometrical mean, dp (μm)	V_g (m s ⁻¹)*	Concentration (μg m ⁻³)	Deposition flux (mg m ⁻² day ⁻¹)
< 0.10 (0.02–0.1)	0.04	2.7×10^{-7}	16.9	4×10^{-4}
0.30–0.10	0.17	1.7×10^{-6}	9.4	1.4×10^{-3}
0.50–0.30	0.38	6.2×10^{-6}	5.6	3×10^{-3}
0.75–0.50	0.61	1.4×10^{-5}	5.6	6.8×10^{-3}
1.13–0.75	0.92	2.9×10^{-5}	7.5	1.9×10^{-2}
2.23–1.13	1.65	8.8×10^{-5}	20.7	0.16
5.47–2.23	3.49	3.7×10^{-4}	9.4	0.30
7.38–5.47	6.35	1.2×10^{-3}	1.8	0.19
11.2–7.38	9.09	2.4×10^{-3}	1.8	0.40
15.1–11.2	13	5×10^{-3}	1.8	0.81
21.3–15.1	17.93	9.5×10^{-3}	1.8	1.54
> 21.3 (21.3–40)	29.18	2.5×10^{-2}	5.6	12.26
Total	15.72			

* v_g is gravitational settling velocity calculated using Eqs. (3) and (4)

Fig. 2 Size fractionated, total PAHs concentration (monthly average, ng m^{-3}) in ambient air associated with the particulate phase



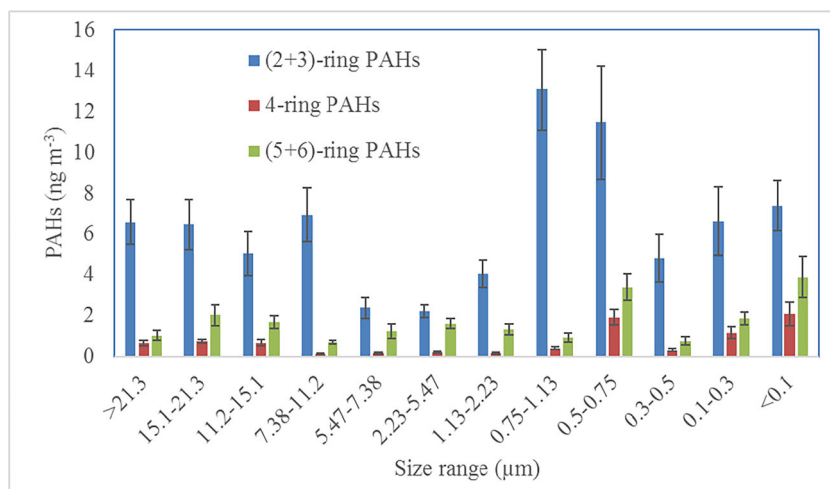
19.3%, respectively, in overall size fractions. The abundance of 5 + 6-ring PAHs was highest in the fine size fraction of PM which could be due to the preferential condensation of less volatile PAH species on fine particles and inhibition of more volatile ones on smaller particles, which is attributed to the Kelvin effect (Hien et al. 2007; Lv et al. 2016).

Filippo et al. (2010) and Kawanaka et al. (2004) had observed a unimodal distribution of PAHs with a peak at $0.48 \mu\text{m}$. For these studies, samplings performed in Rome and Saitama, Japan, respectively, were averaged over a long sampling period (Kawanaka et al. 2004; Filippo et al. 2010). In our study, the peak PAH concentrations were observed at $0.5\text{--}0.75 \mu\text{m}$ fraction, which is slightly higher than that reported in the aforementioned studies. Such observation may occur due to different pollutant sources at the sampling site or differences in air chemistry. For example, the high moisture content in Mumbai air may cause such a discrepancy. A study from Ho Chi Minh City, Vietnam, reports particle size distributions of investigated PAHs were bi-modal with one peak in fine particle mode ($<2.1 \mu\text{m}$) and another in the coarse particle mode ($>2.1 \mu\text{m}$) (Hien et al. 2007). We also have

observed peaked PAH concentration in coarse mode (Fig. 3), especially for two- and three-ring PAHs.

Molecular diagnostic ratios (MDRs)—the ratios of defined pairs of individual compounds—have been widely used as markers of different source categories of polycyclic aromatic hydrocarbons (PAHs) (Katsoyiannis et al. 2011). This approach was used for the identification of contributory sources of PAHs in air-born PM. Three MDRs were used, namely, (1) [FLUO (fluoranthene)/FLUO + PYR (pyrene)], (2) [IND (indeno[1,2,3-cd] pyrene)/IND + BghiP (benzo[g,h,i]perylene)], and (3) BaP (benzo[a]pyrene)/BghiP. MDRs 1–2 can give information about the petrogenic or pyrogenic origin of PAHs and may highlight whether the combustion material is fuel, grass, coal, or wood. The third MDR is used as an indicator of traffic sources for PAHs (Yunker et al. 2002; Dvorská et al. 2011). The mean value of first MDR was 0.36, which indicates that sources of PAHs are petrogenic or the incomplete combustion of petroleum produced them, i.e., $\text{MDR1} < 0.4$, and from fuel combustion. Similarly, the mean value of MDR2 was 0.06, suggesting again the PAH sources are petrogenic as $\text{MDR2} < 0.2$.

Fig. 3 Ring number wise distribution of PAHs (ng m^{-3}) associated with size-fractionated PM



MDR3 average value found to be 0.22, which indicates there are also non-traffic sources PAHs in the ambient air as MDR3 < 0.6. All three MDR values were calculated using the average concentration of PAHs associated with PM during the sampling period. MDR values were not observed to vary significantly ($p < 0.05$) during the sampling period. Source apportionments using isomer ratios such as MDR are realized to be associated with high uncertainties (Dvorská et al. 2011). As in the present study, only particulate-phase PAHs were collected. It may be noted that the assumption of ratios did not change from source to receptor may be problematic because of the environmental degradation.

Dry deposition flux and deposition velocity of PAHs

The monthly averages of dry deposition fluxes for PAHs are summarized in Table 4. A total of 15 PAHs were identified and quantified in the dry deposition samples. As the dry deposition sample collection time was 15 days, the samples may have undergone some PAH losses due to volatilization, photodegradation, or biological transformation (Terzi and Samara 2005). In contrast to their abundance in PM samples, PAHs were found to be present in the dry deposition samples as well, and both follow a similar trend, i.e., their abundance order was March > April > May. The monthly averaged dry deposition fluxes of PAHs were found to be varying between 1008 and 1160 $\text{ng m}^{-2} \text{month}^{-1}$. The dry deposition flux was higher during the colder month, i.e., March compared to April and May. This could be attributed to the higher atmospheric concentrations of PAHs during this month. Overall, the dry deposition fluxes were comparable to the literature values (Terzi

and Samara, 2005; Golomb et al. 2001). Although different sampling methods have opted for dry deposition gathering, and also different PAHs were targeted, a study of a high-resolution emission inventory from Tianjin, China, reported the time-weighted annual mean flux of PAHs in the dry deposition to be $3.3 \pm 1.8 \mu\text{g m}^{-2} \text{day}^{-1}$ (Li et al. 2010), which is higher than the present study, i.e., 0.03 to 0.04 $\mu\text{g m}^{-2} \text{day}^{-1}$. This significant difference may be due to a higher pollution load in ambient air of sampling area or difference in targeted PAHs, e.g., phenanthrene (the most abundant PAHs), which is not reported in the present study. Previous studies suggest that the PAHs associated with the particulate phase accounted for 39% of the PAHs in the dry deposition, while the remaining 61% is attributed to the gas phase PAHs. Studies also claim that lower molecular weight PAHs have a dominant fraction of dry deposition flux contributed by the gas phase, while the large molecular weight PAHs have more than 94.5% of their dry deposition flux contribution from the particulate phase (Sheu et al. 1997; Odabasi et al. 1999). The order of occurrence of PAHs in dry deposition samples was ACY > ANT > PYR > BkF > ACE > BaA + CHRY > NAP > FLUO > FLU > BghiP > BaP > BbF > PER > IND averaged over sampling period. The PAH profile observed in dry deposition is quite comparable to those reported by other investigators (Shannigrahi et al. 2005; Li et al. 2010).

Dry deposition velocities (v_d) for target PAHs were also calculated from their observed dry deposition flux and ambient air concentration through Eq. (1). Dry deposition fluxes and ambient air PAH concentration averaged over the sampling period were used for calculation of deposition velocity. Figure 4 represents the mean and range of deposition velocity estimated for individual PAHs. The deposition velocities for PAH compounds varied from 10^{-4} to 10^{-3}cm s^{-1} with a mean value of $7.5 \times 10^{-4} \text{cm s}^{-1}$ during the sampling period. These dry deposition velocities of PAHs match with the gravitational settling velocity of particles with aerodynamic diameters in

Table 4 Average and standard deviation of individual PAHs dry deposition fluxes ($\text{ng m}^{-2} \text{month}^{-1}$)

	March	April	May
NAP	55.3 ± 15.3	57.3 ± 1.3	45.3 ± 13.3
ACY	472.6 ± 56.6	386.6 ± 154.6	302 ± 70
FLU	25.3 ± 1.6	39.6 ± 12.8	53.5 ± 26.7
ACE	64 ± 2.6	64 ± 30.6	52 ± 18.6
ANT	112.4 ± 13.4	127.3 ± 33.3	163.6 ± 3.1
FLUO	61.6 ± 1.9	60.6 ± 23.2	32.2 ± 5.1
PYR	118.8 ± 2.4	143.3 ± 50.3	109.8 ± 16.8
BaA + CHR	82.6 ± 5.8	54.8 ± 45.2	32.9 ± 23.4
BbF	28.4 ± 1.5	20.7 ± 8.9	31.4 ± 19.6
BkF	26.8 ± 15.9	74.5 ± 20.9	79.9 ± 15.4
PER	7.1 ± 6.5	32.1 ± 7.6	30.9 ± 6.4
BaP	35.8 ± 3.7	30.7 ± 20.6	31.8 ± 21.8
IND	12.6 ± 1.4	17.8 ± 7	14.9 ± 4.1
BghiP	56.6 ± 12.6	32.6 ± 3.3	27.3 ± 8.6
Total	1160 ± 141	1142 ± 420	1008 ± 253

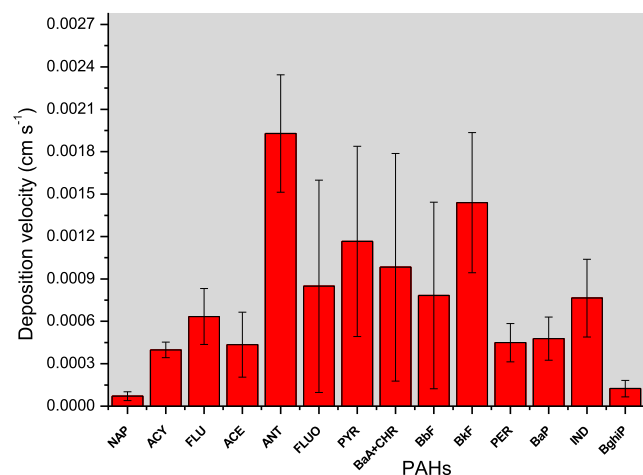


Fig. 4 The dry deposition velocities of individual PAHs, calculated using dry deposition flux and their ambient air concentration

the range of 0.75 to 10 μm (Table 3). For the particle sizes < 0.4 μm and 0.4–1.1 μm , the modeled deposition velocities ($V_{d,i}$) are calculated to be 0.004 cm s^{-1} and 0.037 cm s^{-1} (Sahu et al. 2008), respectively, showing a good agreement with the measured values. Anthracene showed comparatively higher deposition velocity, while for naphthalene, it is minimum. Observed deposition velocities for individual PAHs were smaller than the values reported in the literature (Terzi and Sharma 2005; Sahu et al. 2004; Tasdemir and Esen 2007). Such observations could be due to long dry deposition sampling periods. Moreover, the gas phase concentration of PAHs in ambient air is excluded here, which could cause such discrepancies. Additionally, the small values of dry deposition velocities that were calculated in the present study could be an indication of gas-phase PAHs contributing significantly to the overall dry deposition flux. Gas-phase PAHs are (dry) deposited mainly by a diffusion process, and they have lower dry deposition velocities than the particle-phase PAHs (Sheu et al. 1997). The deposition velocity also depends on the chemical properties of the chemicals, the size of the particles, the characteristics of the receptor surface for dry deposition, and the climatic conditions (Seinfeld and Pandis 2006). The present study site falls in an urban area, where air particles are anticipated to originate primarily from fossil fuels combustion sources; hence, fine PM are expected. The dry deposition velocities of the lower molecular weight PAHs were much lower than the corresponding velocities of the heavier species (Terzi and Sharma 2005).

Metrological parameters and dry deposition

Meteorological parameters measured using an online real-time automatic weather station (Envirotech WM 271, wind monitor) during the sampling period are summarized in Table S4. The monthly average temperature was found to be increasing from March (26 °C) to May (30 °C). As discussed previously, this could be one of the reasons for the decrease in mass concentration from March to May. Variation in other parameters such as wind speed and relative humidity was observed to be minimal during the sampling period, i.e., wind speed ranged from 3.5 to 4 m s^{-1} and relative humidity around 70%. The monthly average dry deposition velocities (0.14, 0.20, and 0.22 cm s^{-1} for March, April, and May, respectively) were found to vary with temperature and other metrological parameters monitored.

Conclusion

Atmospheric size-fractionated PM levels and dry deposition of 15 PAHs were measured at a coastal urban environment of Mumbai, India. Observed PM concentrations during the sampling period were found to be well above the WHO Air

Quality Guidelines. The average dry deposition flux of PM was $12.98 \pm 2.05 \text{ mg m}^{-2} \text{ day}^{-1}$ during the sampling period. A positive linear correlation was observed between mass concentration and dry deposition flux of atmospheric PM. Calculated and observed dry deposition fluxes have shown a positive linear correlation ($r = 0.97$). The monthly trend of PAH concentration was very similar to the PM concentration in ambient air. Most of the \sum_{15} PAHs were associated with fine PM. The values of molecular diagnostic ratios indicated that sources of PAHs in the study area were petrogenic as well as non-traffic. Average monthly dry deposition fluxes of PAHs were found to vary between 1008 and 1160 $\text{ng m}^{-2} \text{ month}^{-1}$. PAH dry deposition velocities values were found equivalent to the particles having aerodynamic diameters in the range of 0.75 to 10 μm . Overall, PAHs associated with PM in the atmosphere were found to follow a very similar trend to that of the PM itself.

Acknowledgments The authors acknowledge Dr. Admir Cr so Targino of Federal University of Technology - Paran /Brazil (UTFPR) for their help in English and content of the present manuscript.

Funding information This work is funded under the plan project of the Government of India at Bhabha Atomic Research Centre.

Compliance with ethical standards

Conflict of interest The authors declare that they have no known competing financial interests or personal relationships that could have appeared to influence the work reported in this paper.

References

- Abdel-Shafya HI, Mansour MSM (2016) A review on polycyclic aromatic hydrocarbons: source, environmental impact, effect on human health and remediation. *Egypt J Pet* 25(1):107–123
- Birg l A, Tasdemir Y, Cindoruk SS (2011) Atmospheric wet and dry deposition of polycyclic aromatic hydrocarbons (PAHs) determined using a modified sampler. *Atmos Res* 101:341–353
- Burkart K, Nehls I, Win T, Endlicher W (2013) The carcinogenic risk and variability of particulate-bound polycyclic aromatic hydrocarbons with consideration of meteorological conditions. *Air Qual Atmos Health* 6:27–38
- Caffery PF (1997) Size distributions, sources, and dry deposition of atmospheric particles in Southern Lake Michigan. Ph.D. Thesis, University of Maryland, College Park
- Chate DM, Rao PSP, Naik MS, Momin GA, Safai PD, Ali K (2003) Scavenging of aerosols and their chemical species by rain. *Atmos Environ* 37:2477–2484
- Cincinelli A, del Bubba M, Martellini T, Gambaro A, Lepri L (2007) Gas-particle concentration and distribution of n-alkanes and polycyclic aromatic hydrocarbons in the atmosphere of Prato (Italy). *Chemosphere* 68(3):472–478
- Connan O, Maro D, He bert D, Roupsard P, Goujon R, Letellier B et al (2013) Wet and dry deposition of particles associated metals (Cd, Pb, Zn, Ni, Hg) in a rural wetland site, Marais Vernier, France. *Atmos Environ* 67:394–403

- CPCB (2009) http://cpcb.nic.in/uploads/National_Ambient_Air_Quality_Standards.pdf (Accessed on April 30; 2019)
- Dvorská A, Lammel G, Klánová J (2011) Use of diagnostic ratios for studying source apportionment and reactivity of ambient polycyclic aromatic hydrocarbons over Central Europe. *Atmos Environ* 45:420–427
- Filippo PD, Riccardi C, Pomata D, Buiarelli F (2010) Concentrations of PAHs, and nitro- and methyl-derivatives associated with a size-segregated urban aerosol. *Atmos Environ* 44:2742–2749
- Garrido A, Jimenez-Guerrero P, Ratola N (2014) Levels, trends and health concerns of atmospheric PAHs in Europe. *Atmos Environ* 99:474–484
- Gnauck T, Muller K, Bruggemann E, Birmili W, Weinhold K, van Pinxteren D, Loschau G, Spindler G, Herrmann H (2011) A study to discriminate local, urban and regional source contributions to the particulate matter concentrations in the city of Dresden, Germany. *J Atmos Chem* 68:199–231
- Golomb D, Barry E, Fischer G, Varanusupakul P, Koleda M, Rooney T (2001) Atmospheric deposition of polycyclic aromatic hydrocarbons near New England coastal waters. *Atmos Environ* 35:6245–6258
- Gupta S, Kumar K, Srivastava A, Srivastava A, Jain VK (2011) Size distribution and source apportionment of polycyclic aromatic hydrocarbons (PAHs) in aerosol particle samples from the atmospheric environment of Delhi, India. *Sci Total Environ* 409:4674–4680
- Hien TT, Thanh LT, Kameda T, Takenaka N, Bandow H (2007) Distribution characteristics of polycyclic aromatic hydrocarbons with particle size in urban aerosols at the roadside in Ho Chi Minh City, Vietnam. *Atmos Environ* 41:1575–1586
- Hussein T, Smolik J, Kerminen V, Kulmala M (2012) Modeling dry deposition of aerosol particles onto rough surfaces. *Aerosol Sci Technol* 46(1):44–59
- IARC (1991) International Agency for Research on Cancer. Monographs on the evaluation of carcinogenic risks to humans. Lyon (FR) 1991: 43–53
- Katsoyiannis A, Sweetman AJ, Jones KC (2011) PAH molecular diagnostic ratios applied to atmospheric sources: a critical evaluation using two decades of source inventory and air concentration data from the UK. *Environmental Science & Technology* 45:8897–8906
- Kaupps H, McLachlan MS (1999) Atmospheric particle size distributions of polychlorinated dibenzo-p-dioxins and dibenzofurans (PCDD/Fs) and polycyclic aromatic hydrocarbons (PAHs) and their implications for wet and dry deposition. *Atmos Environ* 33:85–95
- Kawanaka Y, Matsumoto E, Sakamoto K, Wang N, Yun SJ (2004) Size distributions of mutagenic compounds and mutagenicity in atmospheric particulate matter collected with a low-pressure cascade impactor. *Atmos Environ* 38:2125–2132
- Khairwal R, Sokhi R, Grieken R (2008) Atmospheric polycyclic aromatic hydrocarbons: source attribution, emission factors and regulation. *Atmos Environ* 42:2895–2921
- Kim K, Ara S, Kabir E, Brown RJC (2013) A review of airborne polycyclic aromatic hydrocarbons (PAHs) and their human health effects. *Environ Int* 60:71–80
- Koulouri E, Saarikoski S, Theodosi C, Markaki Z, Gerasopoulos E, Kouvarakis G, Makela T, Hillamo R, Mihalopoulos N (2008) Chemical composition and sources of fine and coarse aerosol particles in the Eastern Mediterranean. *Atmos Environ* 42:6542–6550
- Lee JY, Shin HJ, Bae SY, Kim YP, Kan CH (2008) Seasonal variation of particle size distributions of PAHs at Seoul, Korea. *Air Qual Atmos Health* 1:57–68
- Li X, Tao S, Liu W, Li X, Chen H, Wu S (2010) Dry deposition of polycyclic aromatic hydrocarbons and its influence on surface soil contamination in Tianjin, China. *J Environ Monit* 12:952–957
- Lv Y, Li X, Xu TT, Cheng TT, Yang X, Chen JM, Iinuma Y, Herrmann H (2016) Size distributions of polycyclic aromatic hydrocarbons in urban atmosphere: sorption mechanism and source contributions to respiratory deposition. *Atmos Chem Phys* 16:2971–2983
- Mohan SM (2016) An overview of particulate dry deposition: measuring methods, deposition velocity and controlling factors. *Int J Environ Sci Technol* 13:387–402
- Ncube S, Madikizela L, Cukrowska E, Chimuk L (2018) Recent advances in the adsorbents for isolation of polycyclic aromatic hydrocarbons (PAHs) from environmental sample solutions. *Trends Anal Chem* 99:101–116
- Nsiband SA, Montaseri H, Forbes PBC (2019) Advances in the application of nanomaterial-based sensors for detection of polycyclic aromatic hydrocarbons in aquatic systems. *Trends Anal Chem* 115:52–69
- Odabasi M, Sofuoğlu A, Vardar N, Tasdemir Y, Holsen TM (1999) Measurement of dry deposition and air-water exchange of polycyclic aromatic hydrocarbons with the water surface sampler. *Environ Sci Technol* 33:426–434
- Pacyna JM (2008) Atmospheric deposition. *Ecological Process*:275–285
- Phoothiwut S, Junyapoon S (2013) Size distribution of atmospheric particulates and particulate-bound polycyclic aromatic hydrocarbons and characteristics of PAHs during haze period in Lampang Province, Northern Thailand. *Air Qual Atmos Health* 6:397–405. <https://doi.org/10.1007/s11869-012-0194-3>
- Police S, Sahu SK, Tiwari M, Pandit GG (2018) Chemical composition and source apportionment of PM_{2.5} and PM_{2.5–10} in Trombay (Mumbai, India), a coastal industrial area. *Particuology* 37:143–153
- Pooltawe J, Pimpunchat B, Junyapoon S (2017) Size distribution, characterization and risk assessment of particle-bound polycyclic aromatic hydrocarbons during haze periods in Phayao Province, northern Thailand. *Air Qual Atmos Health* 10:1097–1112
- Pryor S, Gallagher M, Sievering H, Larsen SE, Barthelme RJ, Birsan F, Nemitz E, Rinne J, Kulmala M, Grönholm T (2008) A review of measurement and modelling results of particle atmosphere–surface exchange. *Tellus B* 60:42–75
- Radke M, Willsch H, Welte DH (1980) Preparative hydrocarbon group type determination by automated medium pressure liquid chromatography. *Anal Chem* 52(3):406–411
- Sahu SK, Pandit GG, Puranik VD (2008) Dry deposition of polycyclic aromatic hydrocarbons associated with atmospheric particulate matters in an urban site, Mumbai, India. *Aerosol Air Qual Res* 8(4):437–446
- Sahu SK, Pandit GG and Sadasivan S (2004) Precipitation Scavenging of Polycyclic aromatic hydrocarbons in Mumbai. *Sci Total Environ* 318 (1–3): 245–249.
- Sahu SK, Bhangare RC, Ajmal PY, Sharma S, Pandit GG, Puranik VD (2009) Characterization and quantification of persistent organic pollutants in fly ash from coal fueled thermal power stations in India. *Microchem J* 92:92–96
- Seinfeld JH, Pandis SN (2006) Atmospheric chemistry and physics: from air pollution to climate change, pp 900–931 by John Wiley & Sons, Inc. ISBN-13: 978-0-471-72018-8
- Shahin U, Yi SM, Paodes RD, Holsen T (2010) Long-term elemental dry deposition fluxes measured around Lake Michigan with an automated dry deposition sampler. *Environ Sci Technol* 10(35):1887–1892
- Shannigrahi AS, Fukusima T, Ozaki N (2005) Comparison of different methods for measuring dry deposition fluxes of particulate matter and polycyclic aromatic hydrocarbons (PAHs) in the ambient air. *Atmos Environ* 35:653–662
- Shen G, Wang W, Yang Y, Ding J, Xue M, Min Y, Zhu C, Shen H, Li W, Wang B, Wang R, Wang X, Tao S, Russell AG (2011) Emissions of PAHs from indoor crop residue burning in a typical rural stove: emission factors, size Distributions, and Gas-Particle Partitioning. *Environ Sci Technol* 45:1206–1212
- Sheu HL, Lee WJ, Lin SJ, Fang GC, Chang HC, You WC (1997) Particle-bound PAH content in ambient air. *Environ Pollut* 96(3): 369–382

- Shi JH, Zhang J, Gao HW, Tan SC, Yao XH, Ren JL (2013) Concentration, solubility and deposition flux of atmospheric particulate nutrients over Yellow Sea. *Deep-Sea Res II* 97:43–50
- Shi GL, Zhou XY, Jiang SY, Tian YG, Liu GR, Feng YC, Chen G, Liang YK (2015) Further insights into the composition, source, and toxicity of PAHs in size-resolved particulate matter in a megacity in China. *Environ Chem* 34(3):480–487
- Singh S, Sapra BK, Khan A, Kothalkar PK, Mayya YS (2010) Development of variable configuration cascade impactor for aerosol size distribution measurement. *Atmos Environ* 44:795–802
- Stull RB (2012) *An introduction to boundary layer meteorology*, Springer Science & Business Media, Dordrecht, the Netherlands
- Tasdemir Y, Esen F (2007) Dry deposition fluxes and deposition velocities of PAHs at an urban site in Turkey. *Atmos Environ* 41:1288–1301
- Terzi E, Samara C (2005) Dry deposition of polycyclic aromatic hydrocarbons in urban and rural sites of Western Greece. *Atmos Environ* 39:6261–6270
- Tiwari M, Sahu SK, Bhangare RC, Ajmal PY, Pandit GG (2013) Estimation of polycyclic aromatic hydrocarbons associated with size segregated combustion aerosols generated from household fuels. *Microchem J* 106:79–86
- Tiwari M, Sahu SK, Pandit GG (2017) PAHs in size fractionate mainstream cigarette smoke, predictive deposition and associated inhalation risk. *Aerosol Air Qual Res* 17:176–186
- Tiwari M, Sahu SK, Pandit GG (2017a) Distribution of PAHs in different compartment of creek ecosystem: ecotoxicological concern and human health risk. *Environ Toxicol Pharmacol* 50:58–66
- Tiwari M, Sahu SK, Pandit GG (2019) Environmental distribution and ecotoxicological concerns of phthalic acid esters in creek ecosystem. *J Environ Sci Health A* 54(4):328–336
- Tong X, Chen XC, Chuang HC, Cao JJ, Ho SSH, Lui KH, Ho KF (2019) Characteristics and cytotoxicity of indoor fine particulate matter (PM_{2.5}) and PM_{2.5}-bound polycyclic aromatic hydrocarbons (PAHs) in Hong Kong. *Air Quality, Atmosphere & Health* 12: 1459–1468. <https://doi.org/10.1007/s11869-019-00762-0>
- Wang G, Kawamura K, Xie M, Hu S, Gao S, Cao J, An Z, Wang Z (2009) Size-distributions of n-alkanes, PAHs and hopanes and their sources in the urban, mountain and marine atmospheres over East Asia. *Atmos Chem Phys* 9:8869–8882
- Wang X, Liu S, Zhao J, Zuo Q, Liu W, Li B, Tao S (2014) Deposition flux of aerosol particles and 15 polycyclic aromatic hydrocarbons in the north China plain. *Environ Toxicol Chem* 33(4):753–760
- WHO (2018) [https://www.who.int/news-room/fact-sheets/detail/ambient-\(outdoor\)-air-quality-and-health](https://www.who.int/news-room/fact-sheets/detail/ambient-(outdoor)-air-quality-and-health) ()
- Wu D, Wang Z, Chen J, Kong S, Fu X, Deng H, Shao G, Wu G (2014) Polycyclic aromatic hydrocarbons (PAHs) in atmospheric PM_{2.5} and PM₁₀ at a coal-based industrial city: implication for PAH control at industrial agglomeration regions, China. *Atmos Res* 149:217–229
- Wu Y, Liu J, Zhai J, Cong L, Wang Y, Ma W, Zhang Z, Li C (2018) Comparison of dry and wet deposition of particulate matter in near-surface waters during summer. *PLoS One* 13(6):e0199241. <https://doi.org/10.1371/journal.pone.0199241>
- Yi SM, Totten LA, Thota S, Yan S, Offenbergh JH, Eisenreich SJ, Garney J, Holsen TM (2006) Atmospheric dry deposition of trace elements measured around the urban and industrially impacted NY–NJ harbor. *Atmos Environ* 40:6626–6637
- Yunker MB, Macdonald RW, Vingarzan R, Mitchell RH, Goyette D, Sylvestre S (2002) PAHs in the Fraser river basin: a critical appraisal of PAH ratios as indicators of PAH sources and composition. *Org Geochem* 33:489–515
- Zhang L, Gong S, Padro J, Barrie L (2001) A size-segregated particle dry deposition scheme for an atmospheric aerosol module. *Atmos Environ* 35:49–560
- Zhang K, Zhang BZ, Li SM, Wong CS, Zeng EY (2012) Calculated respiratory exposure to indoor size-fractionated polycyclic aromatic hydrocarbons in an urban environment. *Sci Total Environ* 431:245–251

Publisher's note Springer Nature remains neutral with regard to jurisdictional claims in published maps and institutional affiliations.